Preprint
UCRL-JC-141608

Saturated Plasma X-ray Laser at 19 nm

Y. Li, J. Dunn, J. Nilsen, A. Osterheld, T. W. Barbee Jr., V. N. Shlyaptsev

U.S. Department of Energy

Lawrence Livermore National Laboratory

This article was submitted to *Free Electron Laser Conference 2000, Durham, North Carolina, August 13-18, 2000*

November 30, 2000

This work was performed under the auspices of the United States Department of Energy by the University of California, Lawrence Livermore National Laboratory under contract No. W-7405-Eng-48.

UCRL-JC-141608

Saturated Plasma X-ray Laser at 19 nm

Y. Li[1], J. Dunn[2], J. Nilsen[2], A. Osterheld[2], T. W. Barbee, Jr., and V. N. Shlyaptsev[3]
[1]*Institute of Laser Science and Applications, Lawrence Livermore National Laboratory, Livermore, CA 94550*
[2]*Lawrence Livermore National Laboratory, Livermore, CA 94550*
[3]*Department of Applied Science, University of California at Davis-Livermore, Livermore, CA 94550*

Saturated operation of a tabletop laser plasma X-ray laser at 19 nm is demonstrated with output energy of 2.5 μJ. The narrow beam divergence, high repetition rate, wavelength scalability, short pulse duration, high monochromacity and high brightness make it a potential tool for X-ray laser applications, including seeding a future X-ray free electron laser.

In comparison with other routes towards coherent X-ray sources such as x-ray free electron lasers and high order harmonic generation, plasma X-ray lasers [1] have high output of up to the mJ level and good monochromacity with a bandwidth of the order of 0.01%. This has made them promising tools in many areas of applications such as holography and microscopy of biological structures in the living state, probing of large, dense plasmas relevant to laboratory astrophysics and inertial confinement fusion. They can also be used as the seeds for future accelerator based X-ray free electron lasers operating at fundamental or high harmonics for improving the temporal coherence.

Such plasma X-ray lasers are generated by inducing population inversion in a high temperature high density plasma column with the longitudinal and transverse dimension of ~10 mm and ~0.1×0.1 mm^2. In the case of nickellike Mo studied in this paper, pumping is due to a strong monopole electron collision excitation from the $3d^{10}\ ^1S_0$ ground state to the upper lasing level $3d^9 4d\ ^1S_0$, from which the optical transition back to the ground state is prohibited. A population inversion is generated because the lower lasing state $3d^9 4p\ ^1P_1$ decays rapidly to the ground state via a resonant transition. This then enables lasing at 18.9 nm on the $3d^9 4d\ ^1S_0 \rightarrow 3d^9 4p\ ^1P_1$ transition. Here LS notation is used.

In this paper, we report the demonstration of a laser pumped plasma X-ray laser system using the novel transient collisional excitation (TCE) scheme [2]. The TCE scheme uses a low intensity, long laser pulse (~10^{12}-10^{13} W cm^{-2}, ~ 1 ns) to generate plasma columns from solid targets, which is heated ~1 ns latter by a high intensity, short laser pulse (~10^{15} W cm^{-2}, ~1 ps) to generate the population inversion. The long pulse generates a smooth transverse density profile for the plasma column that allows a better longitudinal propagation of the X-ray laser beam, and the ultrafast heating by the short, intense laser pulse makes it possible to generate unprecedented high gain and enable the X-ray laser to saturate over a small target length.

The saturated operation of the plasma X-ray laser was demonstrated on the compact multipulse terawatt COMET laser system at the Lawrence Livermore National Laboratory [3,4]. The laser occupies two standard optical tables of dimension 1.2 m × 3.6 m. This system is a hybrid CPA laser consisting of a Ti: sapphire oscillator, a regenerative amplifier, and a 4-stage Nd: phosphate glass amplifier. The two final 50-mm diameter amplifiers generate two beams with pulse duration of 600 ps FWHM (full width at half maximum). One of the beams is compressed to generate a short pulse of ~1 ps FWHM duration. The second is sent through a delay line to adjust the delay between the arrivals of the two beams on the target. The two beams were co-aligned to the target chamber where they are focused to form a ~80 μm × 12.5 mm line focus onto solid targets. With the typical energies, the irradiance on the target surface is lower than 10^{12} and 10^{15} W cm^{-2} for the long and the short pulses, respectively. The laser can be fired once every 4 minutes and parameters including energy, pulse shape, pulse separation, near field image and spectrum were monitored.

To make efficient use of the short-lived gain medium, we implemented a travelling wave excitation set-up using a 5-segment stepped mirror which generate group velocity of ~c for the pump laser along the line focus towards the spectrometer, which enhanced the X-ray laser output by up to a factor of 100.

Two diagnostics were used for characterizing the X-ray laser output. One is a time integrating but angularly resolving flat field spectrometer, and the other is a multiplayer mirror imaging system with a magnification of 14.

The x-ray laser output at Ni-like $3d^9 4d\ ^1S_0 \rightarrow 3d^9 4p\ ^1P_1$ 18.9 nm routinely dominates the on-axis spectra [Fig. 1 (a)], and saturation operation of the 18.9 nm X-ray laser was evidenced by its output as a function of the target length [Fig. 1 (b)]. In Fig. 1 (b), the output of the X-ray laser increases nonlinearly with target lengths of up to 8 mm, beyond which the output becomes linear up to target lengths of 10 mm, the maximum target length in this experiment. Fitting to the Linford formula [5], a total gain-length product of ~16.6 is measured, which is a total gain of 1.6×10^6.

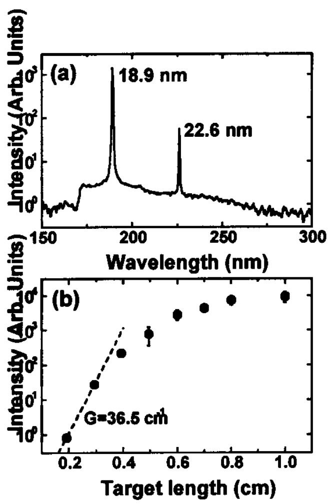

Fig. 1 (a) An on-axis spectrum of the Ni-like Mo X-ray laser from a 10-mm long target, showing the Ni-like 4d $^1S_0 \rightarrow$ 4p $^1P_1$ and 4f $^1P_1 \rightarrow$ 4d $^1P_1$ at 18.9 and 22.6 nm. (b) The Ni-like Mo 18.9 nm X-ray laser output as a function of the target length with an overall gain length product of 16.6. The long pulse and short pulse energy were 1.13 J and 5.02 J, with a delayof 0.7 ns between them. The error bars are due to fluctuation between shots.

We notice that the effective gain decreases continuously with increasing target length before the X-ray laser saturates. The gain starts at 36 cm^{-1} for 3-mm targets and decreases to 5.6 cm^{-1} for 6- to 8- mm targets. We attribute this observation to two facts. The first is the strong spatial variation of the gain coefficients in conjunction with the transverse beam refraction due to the plasma density gradient normal to the target surface. The second is the transient gain lifetime in combination with the non-continuous travelling wave in the experiment. While the refraction deflects the X-ray laser beam from the high-gain, high-density region to the low-gain, low-density region, the segmented travelling wave does not fully utilize the high transient gain with lifetime shorter than the segment length. Both effects deplete the effective gain at long target lengths before the X-ray laser saturates.

The near field beam patterns obtained using the imaging system show typically FWHM of the lasing region of less than 100×100 μm^2. They contains very fine speckle structures, which may be due to the inhomogeneity of the plasma density and gain distribution.

We can also use the imaging system to measure the absolute output of the X-ray laser [6]. The total output energy of the 18.9 nm laser is normally in the range of μJ with the highest being 2.5 μJ. Converting the output energy into intensity using the area of the output aperture and an estimated pulse duration of ~7 ps using previous data with no travelling wave excitation [4], we found the intensity of

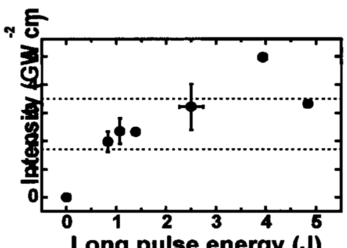

Fig. 2 The 18.9 nm X-ray laser intensity at the output aperture as a function of the long pulse energy at a delay of 0.7 ns and a constant short pulse energy of 5 J. The target length is 1 cm. The dotted lines indicate the range of the theoretical saturation intensities.

the X-ray laser output is normally above 1 GW cm^{-2} (see Fig. 2), and in most of the cases higher than the theoretically estimated saturation intensities of 1.7-3.5 GW cm^{-2}. This further evidenced the saturated operation and robustness of the system.

We have also demonstrated lasing in materials from Ni-like Zr to Sn [4, 7], and Ne-like Ti to Fe, with wavelengths ranging from 14 nm to 33 nm.

In conclusion, we have demonstrated a saturated table-top plasma X-ray laser at 19 nm with output energy of up to 2.4 μJ with picosecond pulse duration and high brightness. Its robustness and scalability in photon energy, and especially the compactness make it a very promising tool for X-ray applications including seeding an X-ray free electron laser.

The authors would like to thank M. Eckart, R. Ward, L. B. Da Silva, and H. Baldis for their support. We thank J. Hunter, B. Sellick, H. Louis, and T. Demiris for technical support. The work was performed under the auspices of the US Department of Energy by the Lawrence Livermore National Laboratory under Contract No. W-7405-Eng-48.

1. R. Elton, X-Ray lasers (Academic Press, New York, 1990).
2. P. V. Nickles, V.N. Shlyaptsev, M. Kalachnikov, M. Schnürer, I. Will, and W. Sandner, Phys. Rev. Lett. 78, 2748 (1997); J. Dunn, A.L. Osterheld, R. Shepherd, W.E. White, V.N. Shlyaptsev, and R.E. Stewart, Phys. Rev. Lett. 80, 2825 (1998).
3. Y. Li, J. Nilsen, J. Dunn, and A. L. Osterheld, A. Ryabtsev, and S. Churilov, Phys. Rev. A 58, R2668 (1998).
4. J. Dunn, J. Nilsen, A. L. Osterheld, Y. Li, and V. N. Shlyaptsev, Opt. Lett. 24, 101 (1999).
5. G. L. Linford, E. R. Peressini, W. R. Sooy, and M. L. Spaeth, Appl. Opt. 13, 379 (1974).
6. Y. Li, J. Dunn, J. Nilsen, A. L. Osterheld, V. N. Shlyaptsev, J. Opt. Soc. Am. B 17, 1098-1101 (2000)
7. J. Dunn, Y. Li, A. L. Osterheld, J. Nilsen, J. R. Hunter, and V. N. Shlyaptsev, Phys Rev Lett 84, 4834-37 (2000).